Radio-frequency spectrum of the Feshbach molecular state to deeply bound molecular states in ultracold ^{40}K Fermi gases

2015 New J. Phys. 17 033013

(http://iopscience.iop.org/1367-2630/17/3/033013)

New Journal of Physics
The open access journal at the forefront of physics

Deutsche Physikalische Gesellschaft DPG
IOP Institute of Physics

Published in partnership with: Deutsche Physikalische Gesellschaft and the Institute of Physics

OPEN ACCESS

RECEIVED
16 November 2014

REVISED
14 January 2015

ACCEPTED FOR PUBLICATION
26 January 2015

PUBLISHED
3 March 2015

PAPER

Radio-frequency spectrum of the Feshbach molecular state to deeply bound molecular states in ultracold ^{40}K Fermi gases

Lianghui Huang[1], Pengjun Wang[1], B P Ruzic[2], Zhengkun Fu[1], Zengming Meng[1], Peng Peng[1], J L Bohn[2] and Jing Zhang[1,3]

[1] State Key Laboratory of Quantum Optics and Quantum Optics Devices, Institute of Opto-Electronics, Shanxi University, Taiyuan 030006, People's Republic of China
[2] JILA, University of Colorado and National Institute of Standards and Technology, Boulder, Colorado 80309-0440, USA
[3] Synergetic Innovation Center of Quantum Information and Quantum Physics, University of Science and Technology of China, Hefei, Anhui 230026, People's Republic of China

Keywords: radio-frequency spectrum, Feshbach molucules, ultracold Fermi gases

Abstract

Spectroscopic measurements are made and obtained for three molecular levels within 50 MHz of the atomic continuum, along with their variation of magnetic field in ultracold ^{40}K Fermi gases. We use spectroscopic measurements to modify the scattering properties near magnetic Fano–Feshbach resonances with a radio-frequency (RF) field by measuring the loss profile versus magnetic field. This work provides the high accuracy locations of ground molecular states near the s-wave Fano–Feshbach resonance, which can be used to study the crossover regime from a Bose–Einstein condensate to a Bardeen–Cooper–Schrieffer superfluid in the presence of an RF field.

The capability to tune the strength of elastic interparticle interactions has led to explosive progress in using ultracold atomic gases to create and explore many-body quantum systems [1]. Magnetic-field-induced Fano–Feshbach resonances are among the most powerful tools for this purpose, and have been used widely in atomic gases of alkali atoms. An alternative technique for tuning interatomic interactions is called optical Feshbach resonance (OFR) [2, 3], in which free atom pairs are coupled to an electronically excited molecular state by a laser field tuned near a photoassociation resonance [4–7]. The OFR offers more flexible control over interaction strength with high spatial and temporal resolution. Furthermore, laser light in combination with magnetic Fano–Feshbach resonances has been developed to modify the interatomic interaction in Bose gases [8–10] and Fermi gases [11].

Radio-frequency (RF) radiation is an appealing alternative means for manipulating ultracold atoms. Note that for alkali atoms, magnetic field Fano–Feshbach resonances may be difficult to find, such as in ^{87}Rb; and that OFRs are problematic in these species because of large losses due to spontaneous emission. Manipulation of scattering lengths via RF radiation therefore represents a powerful new tool. In the context of ultracold gases, RF can be used to couple a two-atom scattering state to a bound molecular state (free-bound coupling) similarly to the OFR. RF can also drive transitions between bound states (bound–bound coupling). As a probe, RF has been used extensively to determine the s-wave scattering length near a Feshbach resonance by directly measuring the RF shift induced by mean-field interactions [12], to demonstrate many-body effects and quantum unitarity [13], and to probe the occupied spectral function of single-particle states and the energy dispersion through Bose–Einstein condensate (BEC)—Bardeen–Cooper–Schrieffer (BCS) crossover [14]. RF can also be considered as a means of controlling scattering length in a variety of scenarios. Zhang *et al* [15] proposed to independently control different scattering lengths in multicomponent gases using RF dressing. The RF coupling of magnetic Fano–Feshbach resonances in a ^{87}Rb Bose gas has been studied experimentally and theoretically [16, 17]. Tscherbul *et al* [18] performed a theoretical analysis of manipulating Feshbach resonances of ^{87}Rb with an RF field. Papoular *et al* [19] suggested using a microwave field to control collisions in atom gases at zero magnetic field. Further, Avdeenkov [20] applied this same idea to manipulate scattering of polar molecules.

In this paper, we experimentally investigate a magnetic Fano–Feshbach resonance in combination with an RF field in ultracold ^{40}K Fermi gases. We measure the spectrum of the nearby molecular bound states with

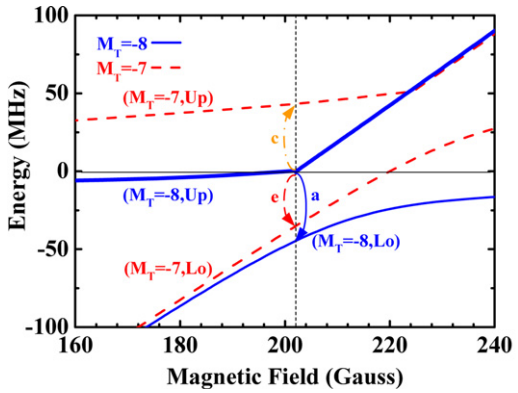

Figure 1. Energy spectrum of relevant molecular levels of $^{40}K_2$ versus the magnetic field in the electronic ground state. The zero of energy is taken to be that of two separated atoms $|9/2, -9/2\rangle + |9/2, -7/2\rangle$ at each magnetic field strength. M_T is total angular momentum projection $M_{F_1} + M_{F_2}$

partial-wave quantum number $L = 0$ by applying a near-resonant RF field. Compared with the s-wave Feshbach molecular state in Bose gas, the Feshbach molecular state in Fermi gas has a longer life time due to the Pauli exclusion principle. We can easily measure the bound-to-bound (Feshbach molecular state to deeply bound molecular states) transitions with an RF field . We can also measure the free-to-bound transitions from free atoms with attractive interaction to these same molecular states. For all three states measured, the binding energies are in good agreement with a theoretical calculation allowing for unambiguous identification of the resonant states. Further, the loss of atoms versus magnetic field is measured, to determine the ability of the RF field to modify scattering. The position of the narrow loss features induced by the RF field in the broad loss profile of magnetic Fano–Feshbach resonances can be changed easily by setting the frequency of the RF field, which represents the modification of the scattering properties near a magnetic Fano–Feshbach resonance, producing resonance features narrower in magnetic field than the original resonance.

We consider potassium 40 atoms in a mixture of hyperfine states $|F, M_F\rangle = |9/2, -9/2\rangle$ and $|9/2, -7/2\rangle$, where F and M_F are the total (electronic plus nuclear) spin, and its projection on the magnetic field axis, respectively. Atoms in such a mixture are known to have an s-wave Fano–Feshbach resonance at a magnetic field $B = 202.2$ G [1]. We consider interspecies collisions between these two states, and their nearby molecular bound states, given in the atom-pair quantum numbers $|F_1, M_{F_1}\rangle|F_2, M_{F_2}\rangle|L, M_L\rangle$, as described in Hund's coupling case (e). Here L and M_L are the quantum numbers of the partial wave angular momentum and its projection. In an ultracold gas, the atoms start in either free pairs with $L = 0$, or else in a very weakly bound Feshbach molecular state with $L = 0$. Since we consider only RF transitions that cannot change L, we omit this index in what follows.

Figure 1 shows the nearby bound s-wave ($L = 0$) molecular levels versus magnetic field, as calculated by a coupled channel model. This model has been engineered to fit simultaneously the s-wave and p-wave Fano–Feshbach resonances reported in [21], and should be a reasonable representation of potassium cold collisions near $B = 200$ Gauss. In this figure the zero of energy corresponds to the threshold energy of the entrance channel $|9/2, -9/2\rangle + |9/2, -7/2\rangle$. The figure shows two molecular bound states ($M_T = -8$, Up and $M_T = -8$, Lo) with total angular momentum projection $M_T \equiv M_{F_1} + M_{F_2} = -8$ (blue solid lines), which exhibit an avoided crossing at the resonance. In the upper curve ($M_T = -8$, Up), the line represents the Feshbach molecule state for $B < B_0$, whereas it becomes a scattering resonance at $B > B_0$. The lower curve ($M_T = -8$, Lo) remains a relatively deeply bound (by ~45 MHz) state in the field range shown. These states can be reached by RF radiation polarized with the magnetic field along the quantization axis set by the magnetic field, satisfying the selection rule $\Delta M_T = 0$. In addition, the figure shows two bound states with $M_T = -7$, which can be reached by RF with perpendicular polarization, with selection rule $\Delta M_T = \pm 1$. The upper ($M_T = -7$, Up) of these bound states is weakly bound with respect to the $|9/2, -9/2\rangle + |9/2, -5/2\rangle$ threshold, and becomes unbound into this continuum at $B \approx 220$ Gauss. The figure also shows arrows (labeled a, c, e) indicating the allowed bound-to-bound transitions that are measured in the experiment.

The experimental apparatus has been described in our previous work [22–25]. The degenerate Fermi gas of about $N \simeq 2 \times 10^6$ ^{40}K atoms in the $|9/2, 9/2\rangle$ internal state is obtained with $T/T_F \simeq 0.3$ by evaporatively sympathetic cooling with bosonic ^{87}Rb atoms in the $|2, 2\rangle$ state inside a crossed optical trap. Here T is the temperature and T_F is the Fermi temperature defined by $T_F = E_F/k_B = (6N)^{1/3}\hbar\bar{\omega}/k_B$ with a geometric mean trapping frequency $\bar{\omega}$. Then a Fermi gas with equal spin-population in the $|9/2, -9/2\rangle$ and $|9/2, -7/2\rangle$ states is prepared at about $B \simeq 219.4$ G. These two hyperfine states form the incoming state $|9/2, -9/2\rangle + |9/2, -7/2\rangle$ in the entrance channel for a pair of atoms, as shown in figure 1. We use a magnetically controlled Fano–

Feshbach resonance at $B_0 = 202.20 \pm 0.02$ G to adiabatically convert a pair of atoms into extremely weakly bound molecules (binding energy <100 kHz).

We place the coil just outside the glass cell and the oscillating magnetic field generated by the RF coil may be parallel (or perpendicular by changing the positions of the RF coil) to the magnetic bias field of the Fano–Feshbach resonance. The RF field is produced by a signal generator (33250A, Agilent). Then the RF radiation passes through an RF switch (ZFSWHA-1-20, Mini-Circuits), is amplified up to 3 W by a power amplifier (ZHL-5W-1, Mini-Circuits) and at last delivered to atoms by a three-turn coil. We apply the RF pulse in a rectangular temporal shape, with variable time that depends on the measurement being made. Near resonance with one of the bound-to-bound transitions, the RF field induces loss in the population of Feshbach molecules due to the excitation to the other molecular states. In order to determine the number of remaining Feshbach molecules in the trap, after turning off the RF, another gaussian-shape RF pulse with duration about 400 μs is applied to dissociate the remaining molecules into free atoms in the state $|9/2, -9/2\rangle + |9/2, -5/2\rangle$. The frequency of the RF pulse used to dissociate Feshbach molecules is fixed to a value that is about E_b larger than the Zeeman splitting between the hyperfine states $|9/2, -7/2\rangle$ and $|9/2, -5/2\rangle$ for the certain magnetic field, which corresponds to the transition from the bound molecules to the free atom state $|9/2, -9/2\rangle + |9/2, -5/2\rangle$. After the dissociation RF pulse, we abruptly turn off the optical trap and magnetic field, and let the atoms ballistically expand for 12 ms in a magnetic field gradient applied along the $\hat{y}$ axis and then take an absorption image along the $\hat{z}$ direction. The atoms in different hyperfine states N_σ ($\sigma = |-7/2\rangle, |-5/2\rangle \ldots$)are spatially separated and analyzed, from which we determine the fraction of molecules $N_{-5/2}/(N_{-5/2} + N_{-7/2})$[4] for different RF frequencies to obtain the spectrum of the bound molecular states.

Figure 2 reports the results of the spectroscopic measurements for the transitions described in figure 1. Figure 2(a) shows the bound-to-bound transition (labeled as 'a' in figure 1) near 45 MHz for different magnetic fields corresponding to different binding energies E_b of the Feshbach molecules. Here the bound molecules are illuminated with the RF pulse duration time of 5 ms and the RF field is parallel to the direction of the magnetic bias field. The lifetimes of Feshbach molecules in the presence of the RF field are measured to be less than 2 ms at $E_b = 30$ kHz, which are much shorter than that without the RF field. When the RF field is perpendicular to the direction of the magnetic bias field, we do not observe any loss of the Feshbach molecules, confirming that the bound state is a state of $M_T = -8$. It is also possible to measure this state starting from a pair of free atoms at $B > B_0$, as shown in figure 2(b), in which we plot the number of atoms remaining after the 50 ms RF pulse. From figures 2(a) and (b), we can know that the larger the binding energy E_b of the Feshbach molecules (on the BEC side) is, the larger the Franck–Condon overlap factor of bound-to-bound transition is. On the other hand, the more the magnetic field keeps away from the Feshbach resonance (on the BCS side), the smaller the Franck–Condon overlap factor of free-to-bound transition is. From these data, we reproduce the binding energy of this state versus magnetic field, which is plotted as the lower data set in figure 2(f), and compared directly to the theoretical calculation (blue line).

Figure 2(c) shows the bound-to-bound transition (labeled as 'c' in figure 1) near 43 MHz for different magnetic fields, corresponding to the transition from Feshbach molecular state to the upper branch molecular state ($M_T = -7$, Up). Again this transition is identified by the energetics of the transition and the slope of transition energy with respect to magnetic field, as computed in the model. The transition can be driven, as expected, by RF radiation of perpendicular polarization, exploiting the selection rule $\Delta M_T = -1$. We also note, to our surprise, that resonant features appear at the same transition frequencies for parallel polarization, with selection rule $\Delta M_T = 0$. The model is unable to identify such a state in the spectrum, and the appearance of these lines in parallel polarization remains a mystery. This state can also be identified in free-to-bound spectroscopy for magnetic fields above $B_0 = 202.2$ G, figure 2(d). Comparing with the theoretical calculation, the measured bound-to-bound (free-to-bound) transition corresponds to the transitions near 43 MHz from the Feshbach molecular state (free atoms) to the upper branch molecular state ($M_T = -7$, Up) as shown in the upper data set in figure 2(f). Note that the resonant position (43.35 MHz) of the free-to-bound spectra for the magnetic bias field 202.5 G in figure 2(d) corresponds to the narrow dip in figure 2(b) with the same magnetic bias field, since both transitions are nearly degenerate at this field.

We have also identified the lower branch molecular state ($M_T = -7$, Lo). However, we cannot observe this state via loss of the Feshbach molecules, even when applying the maximum power of the RF field in our experimental setup, either in perpendicular or parallel polarization. This is presumably because of a comparatively small Franck–Condon overlap between the states. However, one can use a pair of laser beams to coherently couple two bound molecular states via a common electronically excited molecular state (two-color

[4] Here, the fraction of molecules F_{mol} is defined as $2N_{mol}/(N_{-7/2} + N_{-9/2} + 2N_{mol})$. Since $N_{-7/2}$ is equal to $N_{-9/2}$, the fraction of molecules becomes $F_{mol} = N_{mol}/(N_{-7/2} + N_{mol})$. We use the RF dissociation technology (from the bound molecules to the free atom state $|9/2, -9/2\rangle + |9/2, -5/2\rangle$) to measure bound molecular number. The measured bound molecular is $N_{mol}^{mea} = N_{-5/2} = \eta^* N_{mol}$, where η is the detection efficiency of bound molecular. Thus the fraction of molecules can be redefined $F'_{mol} = N_{-5/2}/(N_{-7/2} + N_{-5/2})$.

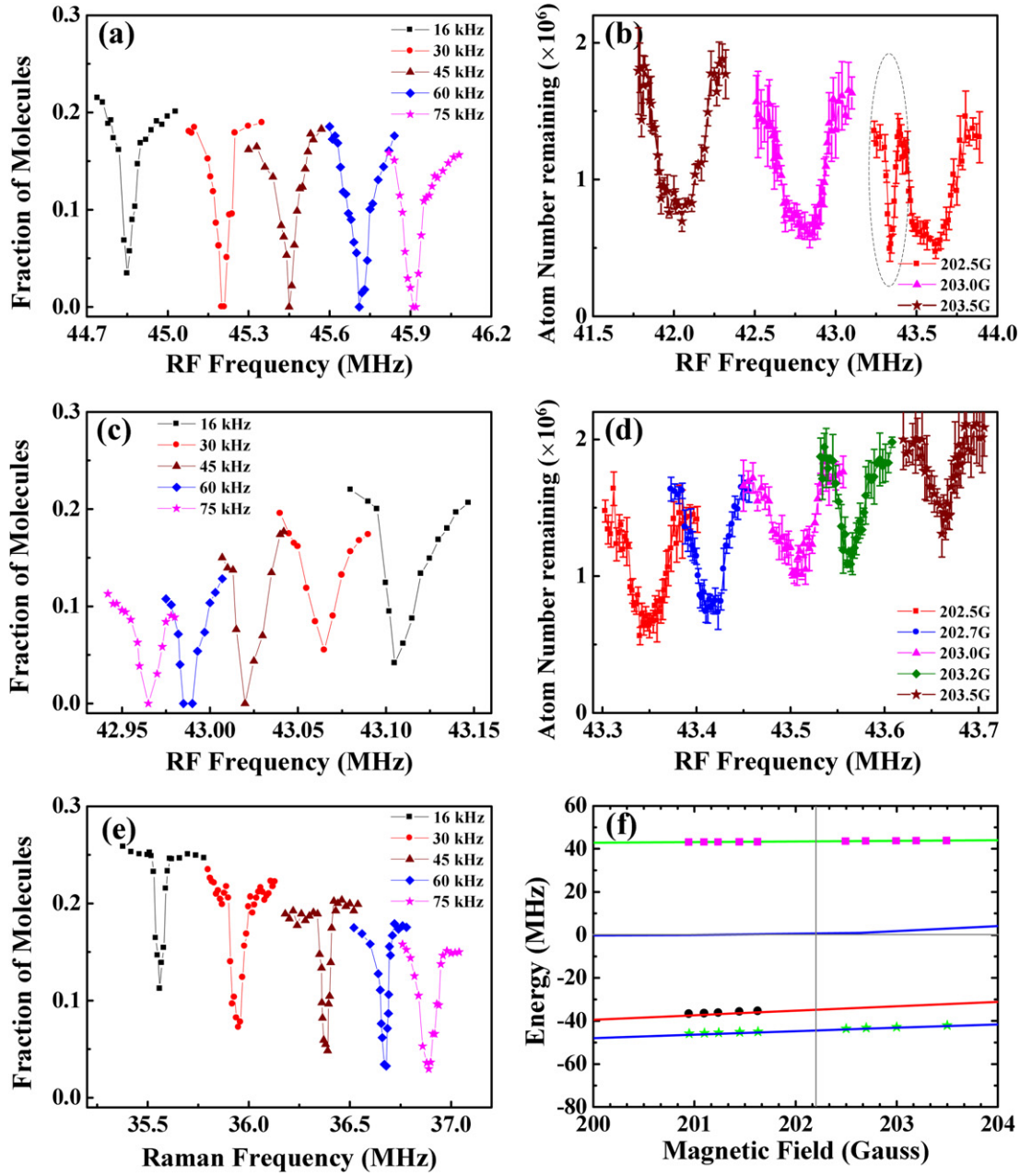

Figure 2. Bound-to-bound and free-to-bound spectroscopy of ground $^{40}K_2$ molecules for different magnetic fields. (a) The bound-to-bound spectroscopy from the Feshbach molecular state to the deeply bound molecular state ($M_T = -8$, *Lo*). (b) The free-to-bound spectroscopy from the free atom to the deeply bound molecular state ($M_T = -8$, *Lo*). The narrow loss dip inside a circle corresponds to the narrow dip in (d) with the same magnetic bias field 202.5 G. (c) The bound-to-bound spectroscopy from the Feshbach molecular state to the deeply bound molecular state ($M_T = -7$, *Up*). (d) The free-to-bound spectroscopy from the free atom to the deeply bound molecular state ($M_T = -7$, *Up*). (e) The bound-to-bound spectroscopy of deeply bound molecular state ($M_T = -7$, *Lo*) for different magnetic fields, which is obtained by a two-color stimulated Raman process. (f) The energies of the deeply bound molecular state as the function of the magnetic field are obtained from (a)–(e). The dot points are the experimental data and the solid lines are obtained from theoretical calculation. The binding energies E_b of 16, 30, 45, 60, and 75 kHz correspond to the magnetic fields of 201.63, 201.45, 201.24. 201.1, and 200.95 G, respectively.

stimulated Raman process) to enhance the coupling between two ground bound–bound molecular states. Here, we carefully choose the one photon detuning of the Raman lasers (wavelength 772.4 nm) to avoid loss due to a Feshbach resonance induced by the laser between the ground Feshbach molecular state and the electronically excited molecular state [11, 26]. The configuration of the two Raman lasers has been described in our previous work [27]. Using these Raman lasers we measure bound-to-bound spectroscopy for ground $^{40}K_2$ molecules near 36 MHz for different magnetic fields, as shown in figure 2(e). These binding energies compare with the theoretical model, as shown by the red line in figure 2(f).

We now consider how the Fano–Feshbach resonance is modified in the presence of the RF field. We do this by measuring the loss profile versus magnetic field, for various RF couplings. Two spin mixture states

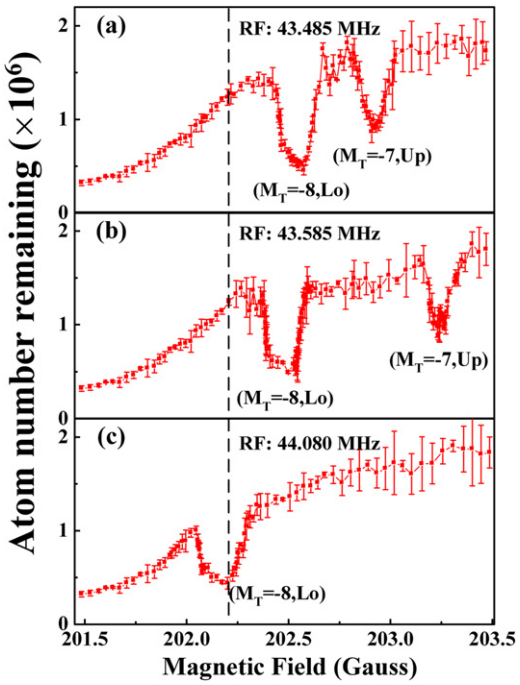

Figure 3. Atom loss from the entrance channel$|9/2, -9/2\rangle$, $|9/2, -7/2\rangle$ in the vicinity of the Feshbach resonance 202.2 G for different frequencies of the RF field. (a) The frequency of the RF field is 43.485 MHz. (b) 43.585 MHz. (c) 44.080 MHz.

$|9/2, -9/2\rangle$ and$|9/2, -7/2\rangle$ are initially prepared at the magnetic field of 210 G and then the field is ramped quickly to its final value within 3 ms. Then the atoms are illuminated with the RF pulse for 50 ms with the RF field polarized parallel to the direction of the magnetic bias field. After this, the remaining atom number is counted by absorption image.

The resulting loss profiles as functions of the magnetic field for the different RF frequencies are shown in figure 3. The broad s-wave Fano–Feshbach resonance of two spin mixture states$|9/2, -9/2\rangle$ and$|9/2, -7/2\rangle$ is at $B_0 = 202.2$ G with a width of 7.04 G [21], as shown in figure 3 for the broad loss profile. The maximum atom loss is not centered on this resonance, but rather occurs at lower-field regions of the spectrum (the BEC side of resonance). The main loss occurs where the Feshbach molecular state is already quite deeply bound [28–30] in sharp contrast with the bosonic case, where maximum loss is observed primarily on the resonance [31–33].

The narrow loss features appear in the broad loss profile when the RF field is applied, which we attribute to transitions 'a' and 'c' in figure 1, namely, transitions to the bound states ($M_T = -8$, Lo) and ($M_T = -7$, Up). The former moves to a lower magnetic field as the RF frequency is increased, while the latter moves to a higher magnetic field, as described by the energies of these resonances. At the RF frequency of 44.080 MHz, the 'a' resonant transition coincides in the magnetic field at $B = 202.2$ G. In this case the naturally occurring magnetic Fano–Feshbach resonance and the RF-coupled bound state can interfere with one another, which can lead, in principle, to a dark state where the atom loss is minimized. These easily discernible features in the loss spectrum are connected with additional resonance scattering, implying that the scattering length is changing [17]. The ability to move these RF resonances with respect to the Fano–Feshbach resonance implies the possibility of creating resonant scattering lengths with a controlled background. Thus this shows that RF radiation may be used to place narrow resonances at any desired magnetic field (which means to locate on a desired position on a broad magnetic Fano–Feshbach resonance), opening new prospects for control of collisions.

In conclusion, we perform the spectroscopic measurement of the Feshbach molecular state to deeply bound molecular states with an RF field in ultracold ^{40}K Fermi gases. This measurement can be used for controlling a magnetic-field Fano–Feshbach resonance by an RF field in ultracold atomic Fermi gases. In the future, when further improving the stability of magnetic fields, we may measure the Rabi oscillation between the Feshbach molecular state and the deeply bound molecular state for the precise control of the scattering length. Since RF radiation is easily manipulated, this technology could be used to switch scattering lengths rapidly and precisely. The tunability of interatomic interactions, as demonstrated in this work, provides a new way to explore the fascinating quantum many-body system of strongly interacting Fermi gases.

Acknowledgments

This research is supported by the National Basic Research Program of China (Grant No. 2011CB921601), NSFC (Grant No. 11234008, 11361161002, 11474188), Natural Science Foundation of Shanxi Province (Grant No.2014011008.2) and Doctoral Program Foundation of the Ministry of Education China (Grant No. 20111401130001). BPR and JLB acknowledge funding from an AFOSR MURI grant.

References

[1] Chin C, Grimm R, Julienne P and Tiesinga E 2010 Feshbach resonances in ultracold gases *Rev. Mod. Phys.* **82** 1225
[2] Fedichev P O, Kagan Y, Shlyapnikov G V and Walraven J T M 1996 Influence of nearly resonant light on the scattering length in low-temperature atomic gases *Phys. Rev. Lett.* **77** 2913
[3] Bohn J L and Julienne P S 1999 Semianalytic theory of laser-assisted resonant cold collisions *Phys. Rev.* A **60** 414
[4] Enomoto K, Kasa K, Kitagawa M and Takahashi Y 2008 Optical Feshbach resonance using the intercombination transition *Phys. Rev. Lett.* **101** 203201
[5] Yamazaki R, Taie S, Sugawa S and Takahashi Y 2010 Submicron spatial modulation of an interatomic interaction in a Bose–Einstein condensate *Phys. Rev. Lett.* **105** 050405
[6] Blatt S, Nicholson T L, Bloom B J, Williams J R, Thomsen J W, Julienne P S and Ye J 2011 Measurement of optical Feshbach resonances in an ideal gas *Phys. Rev. Lett.* **107** 073202
[7] Yan M, DeSalvo B J, Ramachandhran B, Pu H and Killian T C 2013 Controlling condensate collapse and expansion with an optical Feshbach resonance *Phys. Rev. Lett.* **110** 123201
[8] Junker M, Dries D, Welford C, Hitchcock J, Chen Y P and Hulet R G 2008 Photoassociation of a Bose–Einstein Condensate near a Feshbach Resonance *Phys. Rev. Lett.* **101** 060406
[9] Bauer D M, Lettner M, Vo C, Rempe G and Durr S 2009 Control of a magnetic Feshbach resonance with laser light *Nat. Phys.* **5** 339
[10] Bauer D M, Lettner M, Vo C, Rempe G and Durr S 2009 Combination of a magnetic Feshbach resonance and an optical bound-to-bound transition *Phys. Rev.* A **79** 062713
[11] Fu Z, Wang P, Huang L, Meng Z, Hu H and Zhang J 2013 Optical control of a magnetic Feshbach resonance in an ultracold Fermi gas *Phys. Rev.* A **88** 041601
[12] Regal C A and Jin D S 2003 Measurement of positive and negative scattering lengths in a Fermi gas of atoms *Phys. Rev. Lett.* **90** 230404
[13] Gupta S, Hadzibabic Z, Zwierlein M W, Stan C A, Dieckmann K, Schunck C H, van Kempen E G M, Verhaar B J and Ketterle W 2003 Radio-frequency spectroscopy of ultracold fermions *Science* **300** 1723
[14] Stewart J T, Gaebler J P and Jin D S 2008 Using photoemission spectroscopy to probe a strongly interacting Fermi gas *Nature* **454** 744
[15] Zhang P, Naidon P and Ueda M 2009 Independent control of scattering lengths in multicomponent quantum gases *Phys. Rev. Lett.* **103** 133202
[16] Kaufman A M, Anderson R P, Hanna T M, Tiesinga E, Julienne P S and Hall D S 2009 Radio-frequency dressing of multiple Feshbach resonances *Phys. Rev.* A **80** 050701
[17] Hanna T M, Tiesinga E and Julienne P S 2010 Creation and manipulation of Feshbach resonances with radiofrequency radiation *New J. Phys.* **12** 083031
[18] Tscherbul T V, Calarco T, Lesanovsky I, Krems R V, Dalgarno A and Schmiedmayer J 2010 Rf-field-induced Feshbach resonances *Phys. Rev.* A **81** 050701
[19] Papoular D J, Shlyapnikov G V and Dalibard J 2010 Microwave-induced Fano–Feshbach resonances *Phys. Rev.* A **81** 041603
[20] Avdeenkov A V 2012 Dipolar collisions of ultracold polar molecules in a microwave field *Phys. Rev.* A **86** 022707
[21] Gaebler J P, Stewart J T, Drake T E, Jin D S, Perali A, Pieri P and Strinati G C 2010 Observation of pseudogap behaviour in a strongly interacting Fermi gas *Nat. Phys.* **6** 569
[22] Xiong D, Chen H, Wang P, Yu X, Gao F and Zhang J 2008 Quantum degenerate Fermi–Bose mixtures of ^{40}K and ^{87}*Rb* atoms in a quadrupole-Ioffe configuration trap *Chin. Phys. Lett.* **25** 843
[23] Xiong D, Wang P, Fu Z and Zhang J 2010 Transport of Bose–Einstein condensate in QUIC trap and separation of trapping spin states *Opt. Express* **18** 1649
[24] Xiong D, Wang P, Fu Z, Chai S and Zhang J 2010 Evaporative cooling of ^{87}*Rb* atoms into Bose-Einstein condensate in an optical dipole trap *Chin. Opt. Lett.* **8** 627
[25] Wang P, Deng L, Hagley E W, Fu Z, Chai S and Zhang J 2011 Observation of collective atomic recoil motion in a degenerate fermion gas *Phys. Rev. Lett.* **106** 210401
[26] Fu Z, Huang L, Meng Z, Wang P, Liu X J, Pu H, Hu H and Zhang J 2013 Radio-frequency spectroscopy of a strongly interacting spin–orbit-coupled Fermi gas *Phys. Rev.* A **87** 053619
[27] Fu Z, Huang L, Meng Z, Wang P, Zhang L, Zhang S, Zhai H, Zhang P and Zhang J 2014 Production of Feshbach molecules induced by spin orbit coupling in Fermi gases *Nat. Phys.* **10** 110
[28] Dieckmann K, Stan C A, Gupta S, Hadzibabic Z, Schunck C H and Ketterle W 2002 Decay of an ultracold fermionic lithium gas near a Feshbach resonance *Phys. Rev. Lett.* **89** 203201
[29] Bourdel T, Cubizolles J, Khaykovich L, Magalhaes K M F, Kokkelmans S J J M F, Shlyapnikov G V and Salomon C 2003 Measurement of the interaction energy near a Feshbach resonance in a ^{6}Li Fermi gas *Phys. Rev. Lett.* **91** 020402
[30] Regal C A, Greiner M and Jin D S 2004 Lifetime of molecule-atom mixtures near a Feshbach resonance in ^{40}K *Phys. Rev. Lett.* **92** 083201
[31] Roberts J L, Claussen N R, Cornish S L and Wieman C E 2000 Magnetic field dependence of ultracold inelastic collisions near a Feshbach resonance *Phys. Rev. Lett.* **85** 728
[32] Marte A, Volz T, Schuster J, Durr S, Rempe G, van Kempen E G M and Verhaar B J 2002 Feshbach resonances in rubidium 87: Precision measurement and analysis *Phys. Rev. Lett.* **89** 283202
[33] Weber T, Herbig J, Mark M, Nagerl H C and Grimm R 2003 Bose–Einstein condensation of cesium *Science* **299** 232